

physical discussion will be published in a separate paper (Guarnieri et al., 1994).

Acknowledgements

We would like to thank the ESO organization for the allocation of observing time and for giving us the chance to be the first IRAC2 users. We also thank Hans Gemperlein for the help during the observing run. MDG acknowledges the Università and Osservatorio Astronomico of Torino for their support.

References

Arribas, S., Martinez Roger, C., 1987, *AA* **178**, 106.
Bertelli, G., Bressan, A., Chiosi, C., Fagotto, F., Nasi, E., 1994, *AAS* **106**, 275.

Bica, E., Barbuy, B., Ortolani, S. 1991, *ApJ* **382**, L15.
Blackwell, D.E., Shallis, M.J., 1977, *MNRAS* **180**, 177.
Blackwell, D.E., Pedford, A.D., Shallis, M.J., 1980, *AA* **82**, 249.
Buonanno, R., Corsi, C.E., De Biase, G.A., Ferraro, I., 1979, in *Image processing in Astronomy*, eds. G. Sedmak, M. Capaccioli and R.J. Allen, Trieste Obs., p.354.
Buonanno, R., Buscema, G., Corsi, C.E., Ferraro, I., Iannicola, G., 1983, *AA* **126**, 278.
Ferraro, F.R., Fusi Pecci, F., Guarnieri, M.D., Moneti, A., Origlia, L., Testa, V., 1994, *MNRAS* **266**, 829.
Frogel, J.A., Persson, S.E., Aaronson, M., Matthews, K., 1978, *ApJ* **220**, 75.
Frogel, J.A., Persson, S.E., Cohen, J.G., 1981, *ApJ*, **842**.
Guarnieri, M.D., Fusi Pecci, F., Ferraro, F.R., 1992., *Workshop on Star Clusters and Stellar Evolution*, Teramo 18–20 September 1991, *Mem.S.A.It.* **63**, 117.

Guarnieri, M.D., Montegriffo, P., Ortolani, S., Moneti, A., Barbuy, A., Bica, E., 1994, in preparation.
Moorwood A., Finger G., Biereichel P., Delabre B., Van Dijsselendonk A., Huster G., Lizon J.-L., Meyer M., Gemperlein H., Moneti A., 1992, *The Messenger*, **69**, 61.
Ortolani, S., Barbuy, B., Bica, E. 1990, *AA* **236**, 362.
Ortolani, S., Bica, E., Barbuy, B. 1991, *AA* **249**, L31.
Ortolani, S., Barbuy, B., Bica, E. 1992, *AAS* **92**, 441.
Ortolani, S., Barbuy, B., Bica, E. 1993a, *AA* **273**, 415.
Ortolani, S., Barbuy, B., Bica, E. 1993b, *AA* **267**, 66.

For further information please contact:
M.D. Guarnieri;
e-mail: MDGUARNIERI@astbo3.bo.astro.it

Observations of the Shoemaker-Levy 9 Impacts on Jupiter at the Swedish-ESO Submillimetre Telescope

D. BOCKELEEE-MORVAN¹, P. COLOM¹, D. DESPOIS², E. LELLOUCH¹, D. GAUTIER¹, A. MARTEN¹, J. CROVISIER¹, T. ENCRENAZ¹, T. OWEN³

¹Observatoire de Paris-Meudon, France; ²Observatoire de Bordeaux, France; ³University of Hawaii, USA

1. Introduction

The SEST was one of the ten telescopes which were used at ESO for the observation of the encounter of comet Shoemaker-Levy 9 with Jupiter (West, 1994). The purpose of these millimetre observations was to search for molecular species which could have been injected or generated by the impacts. Carbon monoxide was detected on July 23 on impact site G+Q+R+S through its J(2–1) line at 230 GHz. CO, which is normally present with a very low abundance in Jupiter's atmosphere, was likely formed by shock chemistry following the impacts. Difficulties in the reduction of the data prevented us from reporting these results with the other ESO preliminary results of this event in the September 1994 issue of *The Messenger*.

2. Observations

The observations at SEST were conducted from July 18 to 23, 1994. They were a part of a global strategy undertaken by a consortium of European, Canadian and US scientists in order to search for molecular species using millimetre heterodyne techniques. As a result of this strategy, observations of various

molecules were made at the IRAM 30-m radio telescope in Spain (Lellouch et al., 1995), at the IRAM millimetre interferometer in France (Wink et al., 1994), with the James Clerk Maxwell Telescope in Hawaii (Marten et al., 1995), and at the SEST. The interest of millimetre heterodyne techniques for planetary observations is the high spectral resolution which allows the detection of narrow molecular lines formed in the stratosphere.

The SEST 15-m antenna is equipped with three heterodyne receivers working in the 80–116 GHz (3-mm receiver), 215–270 GHz (1.3 mm) and 320–360 GHz (0.8 mm) ranges. These receivers were used alternately, depending on weather conditions. We used as backends two spectrometers simultaneously with an 80-kHz resolution (0.1 km/s at 230 GHz) and a 1.4-MHz resolution. In order to reduce the effects of sky and receiver noise fluctuations, the observations were carried out using the "beam switching" method, in which the receiver alternately viewed the impact site and a reference beam position at 2' in azimuth. Because of the relatively large beam width of the telescope (half-power beam width of 15", 23" and 57" at respectively 346, 230 and 86 GHz) with respect to Jupiter's diameter

(38" in July), we found it was not worth tracking exactly in position the impact sites. For the observations performed with the 3-mm receiver, the centre of the planet was pointed. For those at 1.3 and 0.8 mm, five beam positions regularly spaced on the Jupiter disk at the latitude of the impact sites (44° South) were defined for the observations. After the first observing days, each position generally encompassed several impact sites. Particular attention was given to the observation of the large impacts G, H, K, L, Q and R. 2-min scans were recorded.

The observations suffered from poor atmospheric conditions, with an opacity exceeding 0.5 at 230 GHz during the first 4 days. The weather was more cooperative on July 22 and 23, with opacities on the order of 0.35 and 0.25. On July 18, the J(3–2) and J(2–1) rotational lines of CO at respectively 345 and 230 GHz were searched for. Although the detection of millimetre lines of CO and HCN was announced at the IRAM 30-m and JCMT, the weather appeared too bad at ESO to allow detection of these species at SEST, and the three following days were mostly dedicated to an exploratory search of other species, namely ArH⁺, ArH₃⁺, SO₂, HC₃N near 245 GHz, and SiO (86 GHz) and HCO⁺ (89 GHz). On July

22, we searched for the HCN J(3–2) line at 266 GHz and the CO J(2–1) line at 230 GHz. On July 23, the CO J(2–1) line was observed on several impact sites.

The reduction of the data was hampered by baseline ripples caused by standing waves between the primary and secondary reflectors due to the high continuum flux of Jupiter (80 K in antenna temperature in the main beam at 230 GHz). This resulted in strong irregular oscillations in the spectra, and sometimes in spurious features of linewidth comparable to the searched lines. The real time data processing was not facilitated by the rapid and non-linear velocity displacement of the impact sites as Jupiter rotates (17 km/s in 4.5 hours to be compared to linewidths of a few km/s). This effect could only be taken into account afterwards, by making the ap-

propriate velocity corrections before co-adding the individual scans.

3. Results

The reduction lead to the detection of the J(2–1) of CO from the spectra observed on July 23 in the D+G+Q₁+Q₂+R+S complex (Fig. 1). This line was also detected at IRAM 30-m in impact site G on July 18, ten hours after the fall of the responsible cometary fragment. On July 20.82, 20.84, 21.33 and 21.64, fragments Q₂, Q₁, R and S collided with the planet within 7" of impact site G. As a result, the CO observations made at IRAM and SEST the following days on this site encompassed in fact several sites. The observations performed at SEST on July 22 and 23 complement the monitoring performed at IRAM, for which these dates are lacking. In addition, the

line detected at SEST shows distinctly the contribution of at least three sites (G, Q₂ or R, Q₁). This differs from the IRAM observations which, due to a smaller beam width (10.4"), are more sensitive to the tracked impact site.

The formation of millimetre molecular lines in planetary atmospheres has been discussed at length in several papers (e.g. Lellouch et al., 1984; Paubert et al., 1984). Provided the velocity dispersion within the sites is small, the linewidth reflects pressure broadening and provides thus a strong constraint on the level of formation of CO. The width of the line due to impact G (1 km/s) suggests that CO is not present in a detectable amount at altitudes deeper than 0.1 mbar. The contrast of the line is a function of both the temperature structure and the vertical distribution of the abundance of CO. Figure 1 shows the

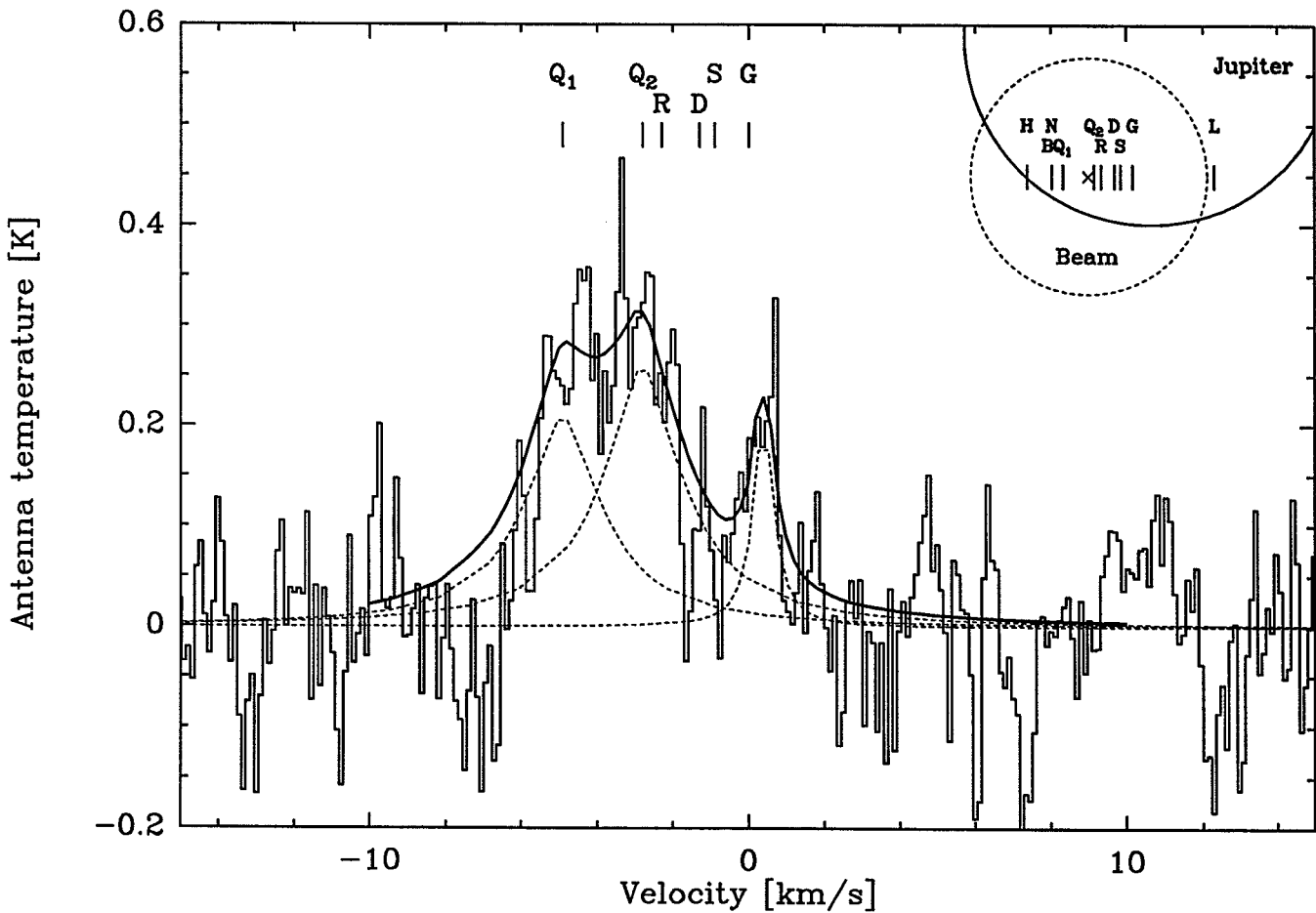


Figure 1: The J(2–1) line of CO at 230.538 GHz detected on site D+G+Q₁+Q₂+R+S on July 23.81 at the SEST telescope. The integration time is 36 minutes. The geometry of the observations is shown in the right upper corner of the figure. Due to the rapid rotation of Jupiter, the geocentric velocities of the impacts differ. The velocity scale refers here to the velocity of impact G. Impact sites D, Q₁, Q₂, R and S were expected at respectively –1.3, –4.9, –2.8, –2.3, and –0.9 km/s at the moment of the observation. Note that the global shape of the line depends critically on the velocity corrections applied before co-adding the individual scans, due to the rapid and non-linear velocity displacement of the impact sites as Jupiter rotates. Superimposed is shown a model fit (full continuous line). Three emitting regions were modeled: Q₁, Q₂ and G (dashed lines). For line calibration, the diameter of each emitting region was assumed to be 2.5" (9400 km). Taking into account the beam efficiency and width, the dilution factor which converts observed antenna temperatures into brightness temperatures is 200. The continuum level originates from the troposphere where the disk-averaged brightness temperature is near 170 K and the opacity is due to H₂–He pressure-induced absorption. For each impact site, we assume a uniform temperature difference relative to pre-impact conditions and a constant CO mixing ratio q_{CO} above a pressure level determined by the linewidths, assumed to be due to pressure-induced collisions. For impact G, we adopt $\Delta T = 30$ K at $p \leq 2$ mbar and $q_{CO} = 4 \times 10^{-5}$ at $p \leq 0.1$ mbar. For impact Q₁, $\Delta T = 30$ K and $q_{CO} = 4 \times 10^{-5}$ at $p \leq 0.4$ mbar. For Q₂, $\Delta T = 40$ K and $q_{CO} = 4 \times 10^{-5}$ at $p \leq 0.4$ mbar. This fit is illustrative, since the solution is from being unique. In particular, impact site R, close to Q₂, was not taken into account. Similar fits can be obtained by assuming increased temperature gradients and lower mixing ratios, and vice versa. The retrieved CO masses are here 1.3×10^{14} g for Q₁ and Q₂, and 3×10^{-13} g for G.

results of model calculations for a multi-site emission. For each impact site, we have assumed emitting region diameters of 2.5" (9400 km), in order to take into account the dilution within the beam. The model parameters are an excess temperature of 30–40 K above the normal 170 K temperature and a CO mixing ratio of 4×10^{-5} above the 0.1 mbar (impact G) or 0.4 mbar (impacts Q₁ and Q₂) levels. This fit is only illustrative and the solution is far from being unique. Emission due to impact R, close to Q₂, was not included. A somewhat higher temperature and lower mixing ratio would equally fit the results, and vice versa. The present solution implies CO masses on the order of 10¹⁴ g for each impact site, consistent with the conclusions of Lellouch et al. (1995) derived from the IRAM data.

4. Discussion

The detection of CO in the stratosphere of Jupiter will provide strong constraints on the physics of the impacts.

CO has normally a very low abundance in Jupiter's atmosphere. The derived abundance is about 50,000 times larger than the normal tropospheric abundance, making unlikely that we were observing jovian CO transported in the plume. Since the high temperatures in the fireball are expected to dissociate most of the cometary and Jovian material, shock chemistry seems to provide the most plausible explanation for the formation of CO. The inferred amount of CO is quite comparable to the oxygen expected in a 1-km sized cometary nucleus. The millimetre observations provide in addition almost unique information on the thermal structure of the Jovian stratosphere modified by the impacts and its temporal evolution. The monitoring of millimetre lines of CO, CS and the HCN line indicated that a substantial warming occurred after the impacts and persisted over one week (Lellouch et al., 1995; Marten et al., 1995). Then the lines switched over from emission to absorption, indicating important cooling down to temperatures lower than the

pre-impact values (Lellouch et al., 1995; Marten et al., 1994, 1995). The SEST observations, together with the other millimetre observations, will help to better understand this unique event.

References

- Lellouch, E., Encrenaz, T., Combes, F., Drossart, P.: 1984, *Astronomy and Astrophysics* **135**, 365-370.
 Lellouch, E., Paubert, G., Moreno, R., Festou, M.C., Bézard, B. et al.: 1995, *Nature* (in press).
 Marten, A., Moreno, R., Paubert, G., Wild, W., Colom, P. et al.: 1994, *BAAS* **26**, 1589–1590.
 Marten, A., Gautier, D., Owen, T., Griffin, M.J., Matthews, H.E. et al.: 1995, *Geophysical Research Letter* (submitted).
 Paubert, G., Gautier, D., and Courtin, R.: 1984 *Icarus*, **60**, 599–612.
 West, R.M.: 1994, *The Messenger*, **77**, 28–31.
 Wink, J., Lucas, R., Guilloteau, S., Dutrey, A.: 1994, *IRAM Newsletter* **18**,

For further information please contact:
 D. Bockelée-Morvan;
 e-mail: Dominique.Bockelee@obspm.fr

Evidence for Diffusely Distributed Dust in Elliptical Galaxies and its Effect on Radial Colour Gradients

P. GOUDFROOIJ, ESO-Garching

The presence of dust in elliptical galaxies has recently been shown to be quite common. Deep optical multi-colour CCD imaging has revealed the presence of dust lanes and patches, and the technique of co-adding IRAS survey scans has led to many detections of elliptical galaxies. The optical and far-infrared surveys reported similar detection rates of dust, which may indicate that dust in elliptical galaxies is generally distributed in the optically detected lanes or patches. However, we show here that the amount of dust as derived from the optical extinction values is typically an order of magnitude smaller than that derived from the IRAS flux densities, in strong contrast with the situation in spiral galaxies. To unriddle this dilemma, we postulate that the majority of the dust in elliptical galaxies exists as a diffusely distributed component which is undetectable using optical methods. Employing a multiple scattering model for the dust, we show that the presence of this newly postulated dust component implies significant radial colour gradients which were essentially thought to arise from stellar population gradients only. The energetics of the diffusely distributed dust component is shown to be consistent with the IRAS data. A comparison of the detectable amount of dust in elliptical galaxies embedded in hot, X-ray-emitting gas with the amount expected in case the production and destruction rates of dust are equal indicates that most of the dust in elliptical galaxies has been accreted from other galaxies.

1. Introduction

Although elliptical galaxies generally do not exhibit the large amounts of interstellar matter (ISM) typically found in spiral galaxies, it has recently become possible to detect various components of the ISM in elliptical galaxies (see, Roberts et al. 1991; Goudfrooij et al. 1994b). These studies have shown that the presence of dust and gas in elliptical galaxies is the rule rather than the exception.

Besides detecting the interstellar matter, we are interested in its origin and fate since this material is expected to hold clues to the formation and subsequent evolution of elliptical galaxies through both the physical properties and the dynamics of the gas and dust. There are at least two possible sources of the observed ISM: accumulation of material shed by evolved, mass-losing giant stars within the galaxy (e.g., Faber & Gallagher 1976; Knapp et al. 1992), and accretion of gas during galaxy interactions.

In order to systematically study the global occurrence and properties of dust and gas in elliptical galaxies, we (P. Goudfrooij from ESO, L. Hansen and H.E. Jørgensen from the Copenhagen University Observatory, H.U. Nørgaard-Nielsen from the Danish Space Research Institute, and T. de Jong from the University of Amsterdam) have performed an optical survey of a complete, *apparent*-magnitude selected sample of elliptical galaxies, containing all such objects (56 in number) with $B_T^0 < 12$ mag. in the *Revised*